3-1-2006

Effects of Rapid Heating on Solutionizing Characteristics of Al-Si-Mg Alloys Using a Fluidized Bed

S. K. Chaudhury

Diran Apelian
Worcester Polytechnic Institute, dapelian@wpi.edu

Effects of Rapid Heating on Solutionizing Characteristics of Al-Si-Mg Alloys Using a Fluidized Bed

S.K. CHAUDHURY and D. APELIAN

Effects of rapid heat transfer using a fluidized bed on the heat-treating response of Al-Si-Mg alloys (both unmodified and Sr modified) were investigated. The heating rate in the fluidized bed is greater than in conventional air convective furnaces. Particle size analyses of eutectic Si showed that the high heating rate during fluidized bed solution heat treatment causes faster fragmentation and spherodization of Si particles compared to conventional air convective furnaces. The mechanism of Si fragmentation through fluidized bed processing is through both brittle fracture and neck formation and its propagation. In contrast to this, the mechanism of Si fragmentation using a conventional air convective furnace is through neck formation and propagation. The Sr-modified D357 alloy showed a faster spherodizing rate than the unmodified alloy. Thermal analyses showed an exothermic reaction during solution heat treatment using a fluidized bed due to recrystallization, and coarsening of eutectic Al grains. Whereas the alloy solutionized using a conventional air convective furnace showed two exothermic reactions, one due to annihilation of point defects and the other due to recrystallization, and coarsening of the eutectic grains in the aluminum matrix. The recrystallization temperature of the alloy solutionized in the fluidized bed is lower than those in the conventional air convective furnace. Both tensile strength and elongation of fluidized bed solutionized alloys are greater than those solutionized using the air convective furnace. The optimum heat-treatment time for T4 temper using a fluidized bed for unmodified and Sr-modified alloy was reduced to 60 and 30 minutes, respectively.

I. INTRODUCTION

INCREASING demands for lightweight metals as structural components in the automotive and aerospace industries have led to the extensive use of Al-Si-Mg–based foundry alloys. One advantage of using lightweight materials is to increase the payload capacity. Al-Si-Mg alloys are candidate materials for such applications due to their good castability characteristics.[1] The addition of Mg makes the alloy heat treatable,[2–6] which helps to tailor mechanical properties by selecting a suitable temper subsequent to casting. The T6 temper is a widely accepted heat-treatment process for aluminum alloys to increase strength. The T6 temper is comprised of solution heat treatment, quenching, and then artificially aging. The solution heat treatment increases ultimate tensile strength and ductility, while aging increases yield strength at the expense of ductility. In the case of the T4 temper (solution heat treatment followed by quenching), the increase in strength is through the solute solution strengthening mechanism (Mg and Si atoms retained in the postquenched state), and the increase in ductility is due to the spherodization of eutectic Si particles. However, the increase in yield strength on aging after T4 temper is through precipitation strengthening owing to the precipitation of Mg_2Si particles. The resultant mechanical properties of the heat-treated alloy depend on its chemical composition.

In addition to Si and Mg, cast Al-Si-Mg alloys usually contain Fe as an impurity element. Depending upon the Mg content, Fe may exist as π phase ($Al_8Mg_3FeSi_6$), as β-Fe needles (Al_5FeSi), as Al_8FeSi, or as a combination of the preceding phases. The solidus temperature of the alloy depends on the iron-rich phase(s). The type and morphology of iron-rich phase(s) that form in Al-Si-Mg alloys depend on the Mg content. It has been observed[3] that iron-rich phase(s) have a different morphology in Al-Si-Mg alloys containing 0.4 pct Mg as compared to those containing 0.7 pct Mg. The former with 0.4 pct Mg, after solution heat treatment, contains only small β-phase plates, whereas the latter (0.7 pct Mg) contain large π phase and a small number of β plates. The morphology of the iron-rich phase has a significant effect on the ductility of these alloys. The reduction in ductility and fracture toughness in alloys with low Mg content is associated with the formation of plate-shaped β phase. In alloys with higher Mg content, the predominant intermetallics are π phase and their effect on ductility is found to be dependent on whether the alloy is Sr modified. It is observed[3] that in Sr-modified alloy containing 0.7 pct Mg, the fraction of cracked π phase is greater than Si, since π phase is much coarser than Si. However, in unmodified alloys, the fraction of cracked Si and π-phase particles are observed to be equal.[3]

In Al-Si-Mg alloys, it has been widely reported that Mg and Si go into solution during solution heat treatment and are retained in the Al matrix on quenching. However, the effect of rapid heating on heat-treatment characteristics has not been closely examined. The heating rate plays a crucial role in increasing the kinetics of metallurgical processes; the effect of rapid heating through a fluidized bed heat treating system (henceforth referred to as FB) on solution heat-treatment characteristics of Al-Si-Mg (D357) alloy is the focus of this study.

Alloy D357 is widely used in aerospace applications; in conventional practice, the alloy is heat treated for about 20 hours using a conventional circulating air convective heat-treating furnace (henceforth referred to as CF). There is a major thrust to reduce the total heat-treatment time and thereby increase

S.K. CHAUDHURY, Research Associate, and D. APELIAN, Director, are with the Metal Processing Institute, Worcester Polytechnic Institute, Worcester, MA 01609. Contact e-mail: sujoy@wpi.edu

Manuscript submitted July 19, 2004.

productivity. With the advent of FB processing, the net heat-treatment time can be reduced by almost an order of magnitude. Previous fluidized bed heat-treatment systems had specific flaws in their design that hindered their use. One such problem was the lack of temperature uniformity in the bed since the fluidizing air was introduced at ambient temperature. A recently developed fluidized bed[7] is distinct in that the fluidizing air is made to flow over the heating element prior to entering the furnace. This ensures minimum heat loss from the bed and excellent temperature uniformity. The maximum temperature variation observed in the laboratory fluidized bed used in this work was ±1 °C to 2 °C. Temperature uniformity within the furnace is a critical issue.

The effect of fluidized bed processing (solution heat treatment and aging) on the resultant microstructure and mechanical properties of unmodified and Sr-modified D357 alloys was investigated. In this article, we studied the effect of solution heat treatment using a fluidized bed on microstructure and tensile properties of alloys. Tensile properties are correlated to microstructural changes, primarily to morphological changes of Si particles during the solution heat treatment. For comparative purposes, alloys were also heat treated using CF, and the resultant microstructure and tensile properties were examined.

II. EXPERIMENTAL PROCEDURE

A. *Alloy Composition*

Alloy D357 was procured from Hitchcock Industries (MN) in the form of cast plates. The chemical composition of the alloy is given in Table I. The chemical composition was measured using the spectrographic technique and is given in weight percentage. In addition to the basic alloying elements (Si and Mg), the alloy also contains Fe as an impurity element. It is well known that the presence of Fe as an impurity element in most Al-Si-Mg based foundry alloys has a deleterious effect on ductility.[8] The Be is added to counter this by spherodizing the Fe-rich intermetallics.[18] The alloy also contains Ti as an alloying element, and its intermetallic (Al_3Ti) is a well-known grain refiner.[9] The heat-treatment characteristics of both unmodified and Sr-modified D357 alloys were studied

B. *Heat Treatment*

Laboratory-type FB was used for solution heat treating and aging. The technical detail of the FB is given in Reference 7. Staurolite sand ($FeAl_5Si_2O_{12}OH$) was used as the fluidized bed material. Its particle size was in the range of 80 to 120 μm and particles were heated to the desired temperature by means of a series of heating elements placed underneath the bed. The temperature variation in the bed was found to be within 1 to 2 °C of the set temperature. For purposes of comparison, parts were also heat treated in a resistance furnace. The cast plates were solution heat-treated using the FB and the CF at different temperatures and for various time intervals. The heat-treatment schedule of the D357 alloy (both unmodified and Sr modified) for T4 treatment (solution heat treating and quenching in water at 25 °C) is shown in Table II. It may be noted that the solution heat-treating temperature selected was based on the solidus temperature of the alloy. The solidus temperature was determined by monitoring the cooling profile (temperature *vs* time) during casting. The first derivative curve was superimposed on the cooling curve to determine the solidus temperature. The solidus temperature reported for D357 alloy is 546 °C. No significant difference was noted with respect to the solidus temperature of the Sr-modified D357 alloy *vis-à-vis* unmodified D357 alloy. The solution heat treatment was carried out at 543 °C. Times given in Table II are the isothermal times, and do not include the ramp-up time, unless stated otherwise. The time delay during quenching was less than 10 seconds. Optimum solution heat-treatment times were obtained using the fluidized bed for unmodified as well as Sr-modified alloy.

Table I. Chemical Composition of Alloys

Alloy	Si	Mg	Fe	Sr	Ti	Be	Al
D357	6.9	0.56	0.06	—	0.18	0.05	balance
D357(Sr)	7.1	0.56	0.07	0.01	0.18	0.05	balance

C. *Thermal Analysis*

Phase transformations of alloy D357 that occur during solution heat treatment were studied using thermal analysis (TA) methods. The TA work was carried out by analyzing the first derivative of the temperature-time profile monitored during heat treatment of the alloy. A phase or physical transformation is accompanied by a release (exothermic) or absorption (endothermic) of thermal energy, which is usually detected by superimposing the first derivative (dT/dt) curve on the heating profile (*i.e.*, temperature (T) *vs* time (t)). An exothermic curve will result in a sudden increase of dT/dt value, whereas an endothermic event results in a sudden decrease of dT/dt value at the point of transformation. Temperature measurements were carried out using DASY Lab view software coupled with a data acquisition system at an acquisition rate of 10 data per second.

D. *Microstructural Observations*

Microstructural characterization of the as-cast and the heat-treated alloys were carried out using both optical microscopy and scanning electron microscopy (SEM). Standard metallographic techniques were adopted for sample preparation. For optical microscopy, samples were ground using SiC paper of different grit size, followed by polishing with alumina powder (0.2 μm) and silica gel (0.05 μm). The morphology (size and shape) of Si particles was measured using image. The least count of the measurement is ±0.1 μm. The shape of particles was quantified by measuring the shape factor (SF), given by

$$SF = P^2/4\pi A$$

where P is the perimeter and A is the area of the particle.

The particle with SF of unity resembles a sphere, and the greater the SF deviates from unity, the less will be the

Table II. Heat-Treatment Schedule for D357 (Both Unmodified and Sr-Modified) Alloy T4 Temper at 543 °C

Processing	Time (min)							
FB	15	30	45	60	90	120	—	—
CF	—	30	—	60	—	120	360	540

sphericity of the particle. Samples for SEM were prepared by electropolishing samples after grinding them on SiC paper (4000 grit size). The electropolishing was performed at 30 V for 20 seconds using a freshly prepared electrolyte, whose composition was 60 pct Ethyl alcohol, 20 pct Perchloric acid, and 20 pct Ethylene glycol by volume. Electropolished samples were then etched with concentric nitric acid for 5 seconds and immediately rinsed in running water. The Nitric acid etching was used to observe Mg_2Si particles in samples under SEM.

E. *Evaluation of Mechanical Properties*

The ultimate tensile strength, yield strength, and elongation of as-cast and heat-treated test bars were measured. Tensile specimens were machined from the as-cast and heat-treated plates. Tensile bars were machined per ASTM standard specification B557 with 1-in. gage length. Tensile properties were measured at a 0.1-in./min extension rate. At least five tests were conducted for each heat-treatment condition and the average value is reported. During tensile tests, some samples fractured prematurely from the neck region due to the presence of inclusion or porosity and gave reduced tensile properties. These results were not included when reporting average values of ultimate tensile strength, elongation, and yield strength.

III. RESULTS AND DISCUSSION

Prior to presenting and discussing the microstructure and mechanical properties of the alloy heat treated to different conditions using the FB and the CF, it is imperative to review the thermodynamic simulation results of Al-Si-Mg alloy, which are pertinent to the heat-treatment response. The phase diagram of the Al-Si-Mg system was simulated using PANDAT software to study the effect of Mg concentration on phase changes during postsolidification heat treatment. The simulation analysis was performed on the Al-Si-Mg based system. Figure 1 shows the effect of Mg concentration on Al-7Si-0.07Fe-0.18Ti alloy. The concentration of Mg was varied from 0.1 to 0.7 wt pct. Phases stable in different regions (marked in Figure 1) of the composition/temperature isopleth are given subsequently:

Region 1: Liquid + Al_3Ti
Region 2: Liquid + Al_3Ti + Al
Region 3: Liquid + Al
Region 4: Liquid + Al + Si
Region 5: Si + Al + β
Region 6: Si + Al + β + Al_3Ti
Region 7: Si + Al + β + π
Region 8: Si + Al + π
Region 9: Si + Al + π + Mg_2Si
Region 10: Si + Al + π + Mg_2Si + Al_3Ti
Region 11: Si + Al + π + β + Al_3Ti
Region 12: Si + Al + β + Mg_2Si + Al_3Ti

The isopleth (Figure 1) can be divided into two regions with regard to its importance to postsolidification heat treatment based on Mg concentration. These are (1) region I with Mg concentrations less than 0.2 pct and (2) region II with Mg concentrations greater than 0.2 pct (as marked by the left- and right-hand side of the dotted line in Figure 1). In the case of Mg concentrations below 0.20 pct, where the phases that are stable at solution heat-treating temperatures between 535 °C and 550 °C are α-Al, Si, and Al_5FeSi (β phase), Mg forms a solid solution in the Al matrix per the equilibrium phase diagram. In contrast, when Mg concentration is greater than 0.20 pct, regions 7 and 8 indicate the phase stability at solution heat-treating temperatures (535 °C to 550 °C). Thus, thermodynamic analysis predicts that solution heat treatment of the Al-Si-Mg-Fe type alloy with Mg concentration greater than 0.2 pct will result in partial dissolution of Mg, since the $Al_8FeMg_3Si_6$ phase is likely to be retained on quenching from the solution heat-treating temperature. In addition, it should be noted that for the alloy with Mg composition in the range of 0.20 to 0.5 pct (region I), the Fe-rich intermetallic phase exists only as a β phase (Reaction [5]) at solution heat treating temperature. However, for Mg content between 0.5 and 0.7 pct, both β and π phases coexist at solution heat-treatment temperatures (region II). The β phase has a faceted morphology with sharp angular edges, and acts as a stress concentrator leading to inferior mechanical properties. In contrast to this, π phase has a Chinese script–like morphology with round edges, and is less harmful than the β phase. The Mg content of Al-Si-Mg alloys is quite critical and plays an important role in microstructural evolution during postsolidification heat treatment.

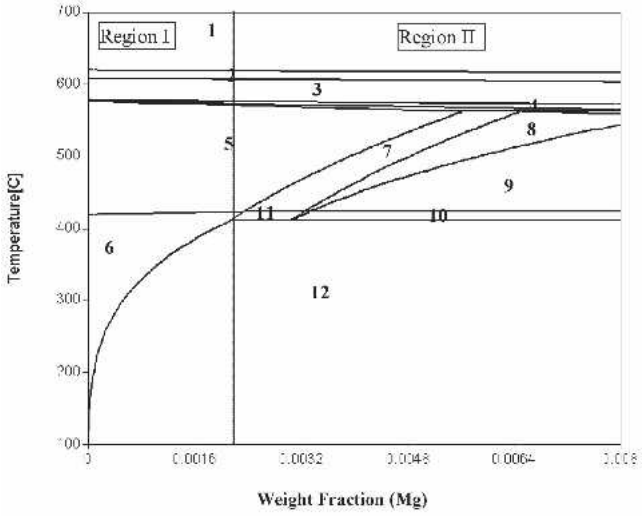

Fig. 1—Phases stable in Al-7Si-0.07Fe-0.18Ti as a function of Mg concentration and temperature in different regions of the isopleth diagram. These regions are as follows: (1) Liquid + Al_3Ti, (2) Liquid + Al_3Ti + Al, (3) Liquid + Al, (4) Liquid + Al + Si, (5) Si + Al + β, (6) Si + Al + β + Al_3Ti, (7) Si + Al + β + π, (8) Si + Al + π, (9) Si + Al + π + Mg_2Si, (10) Si + Al + π + Mg_2Si + Al_3Ti, (11) Si + Al + π + β + Al_3Ti, and (12) Si + Al + β + Mg_2Si + Al_3Ti.

A. *Microstructural Evolution*

In an earlier study,[10,11] it was reported that the heating rate in the FB is an order of magnitude greater than the CF. For a cylindrical aluminum alloy (70-mm long and 38-mm diameter), it took 4 minutes to attain the solution heat-treating temperature, whereas in contrast to this, using a CF, the time required to attain solution heat treating temperatures was

30 minutes. The high heating rate in the FB plays a critical role in the microstructural changes and tensile properties of heat-treated alloys.

There are four important microstructural issues pertaining to solution heat treatment of Al-Si-Mg alloys. These are as follows: (1) dissolution of Mg_2Si particles and retaining solute (Si and Mg) in supersaturated aluminum matrix, (2) fragmentation and spherodization of Si particles, (3) morphological change(s) in Fe-rich intermetallics, and (4) reduction in microsegregation of solutes (Mg and Si) in primary aluminum dendrites. These are discussed subsequently. No direct measurements were made to study the reduction in microsegregation kinetics; however, in previous work by the authors,[10,11] it was observed that microsegregation was significantly reduced in the A356 (Al-7Si-0.3Mg) alloy within 30 minutes of solutionizing using an FB. In another study,[22] Snugovski *et al*. have reported that Si microsegregation in Al matrix can be significantly reduced within 10 minutes of homogenization at 500 °C.

The as-cast microstructures of D357 and Sr-modified D357 alloys are shown in Figures 2(a) and (b) and 3(a) and (b) respectively. The unmodified D357 alloy typically consists of primary aluminum dendrites and irregular distribution of eutectic Si in the interdendritic eutectic region (Figure 2(a)). The Si particles have a flakelike morphology. Deep-etched samples show Si precipitates with faceted morphology in the dendritic region. In addition to this, Fe-rich particles are also observed; the EDX analysis reveals this phase as π phase. The Fe-rich particles have a Chinese script–like morphology and are found in the interdendritic regions; similar microstructures have been observed previously.[4] Though the equilibrium phase diagram predicts the formation of β phase upon solidification, the castings examined show the formation of π phase. This may be due to nonequilibrium solidification, which prevents the transformation of π to β phase, or it may be due to the presence of Be, which can act as a π-phase stabilizer.[18]

The as-cast microstructure also consists of both spherical and needle-shaped Mg_2Si particles at the center of the dendrites. The length of the Mg_2Si needles ranges from 400 to 1200 nm. The periphery of dendrites is devoid of Mg_2Si particles. The segregation of Mg_2Si particles in the center of the dendrite is due to the microsegregation of Mg and Si during solidification. It has been shown[4] that Mg_2Si formation is favorable when the ratio of Mg:Si is 1:1 in the Al lattice. The microsegregation may disturb this ratio and prevents the formation of Mg_2Si particles at the periphery of the dendrites. It should be noted that this ratio is not the bulk ratio of Mg and Si in the alloy. Thermodynamically, it is predicted that due to the microsegregation, concentration of Si and Mg are less at the center and greater at the dendrite periphery. However, some cases of inverse segregation of Si have also been observed.[2] It has been reported[22] that the rapid cooling during solidification resulted in normal segregation, as predicted by solidification theory, whereas slow cooling during casting resulted in the inverse segregation. The inverse segregation of Si at the periphery of dendrites is due to the coarsening of eutectic Si.[2] In addition to Mg_2Si particles, Si precipitates of 1 to 2 μm are also observed in the center of the dendritic region.

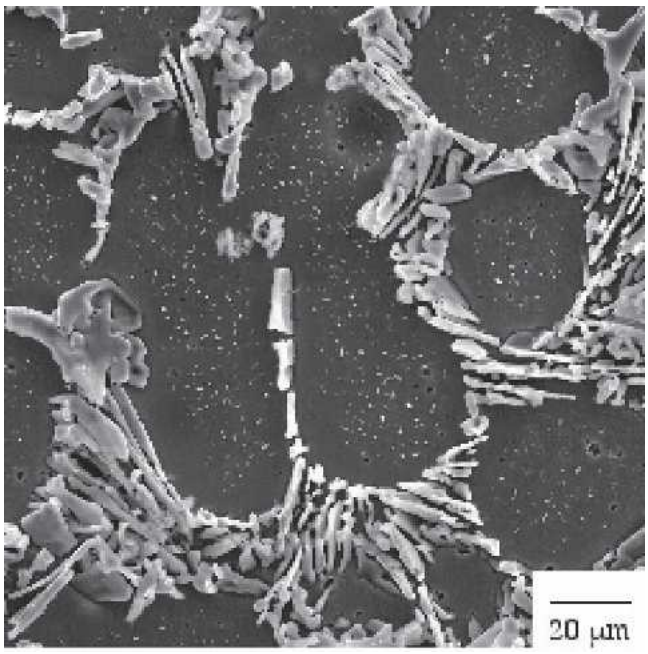

(*a*)

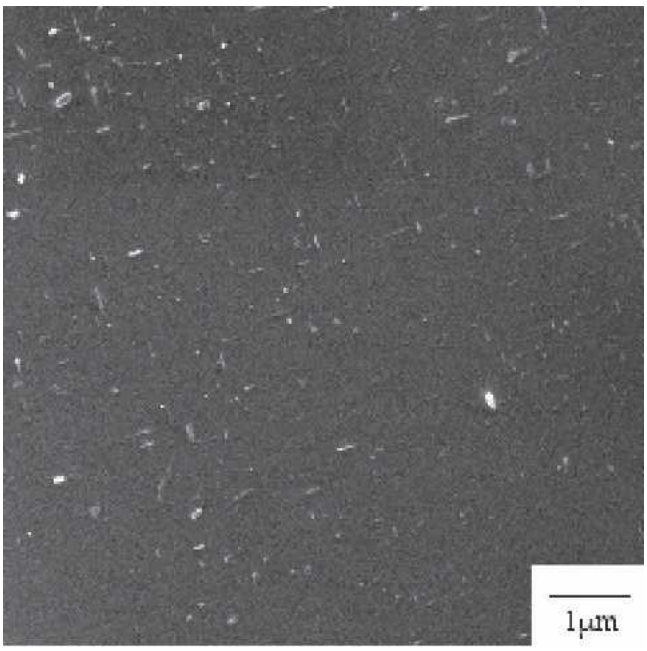

(*b*)

Fig. 2—Micrographs of as-cast unmodified D357 alloy showing (*a*) eutectic Si structure and (*b*) Mg_2Si needles in the dendritic region of the Al matrix.

The microstructure of as-cast Sr-modified D357 alloy is shown in Figures 3(a) and (b). The morphology of Si is mostly fibrous. However, at the periphery of the dendrite, refined flakelike morphologies were observed. It may be noted that the Si particles at the periphery of the dendrites are the first to nucleate and do not resemble a modified structure. The reason for the formation of refined flakelike morphology in Sr-modified alloy at the periphery of the dendrites is not clear. The presence of Sr has no significant effect on the formation of the Mg_2Si phase; the latter has a mostly

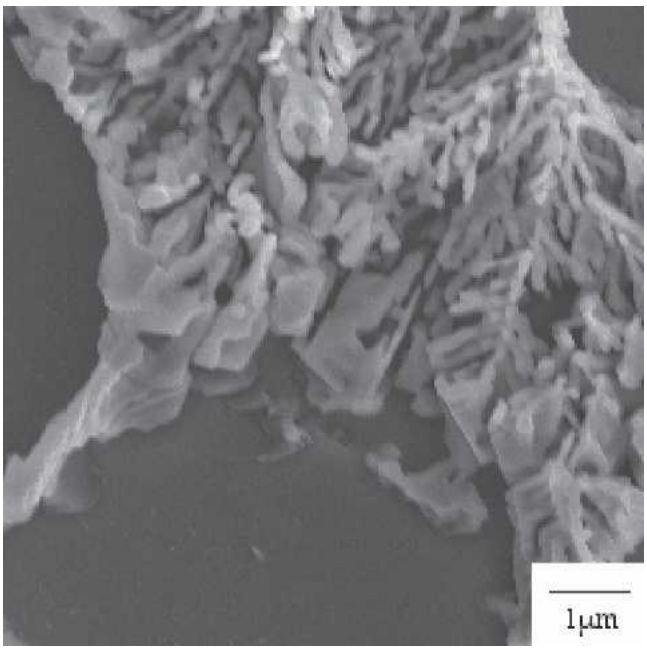

(*a*)

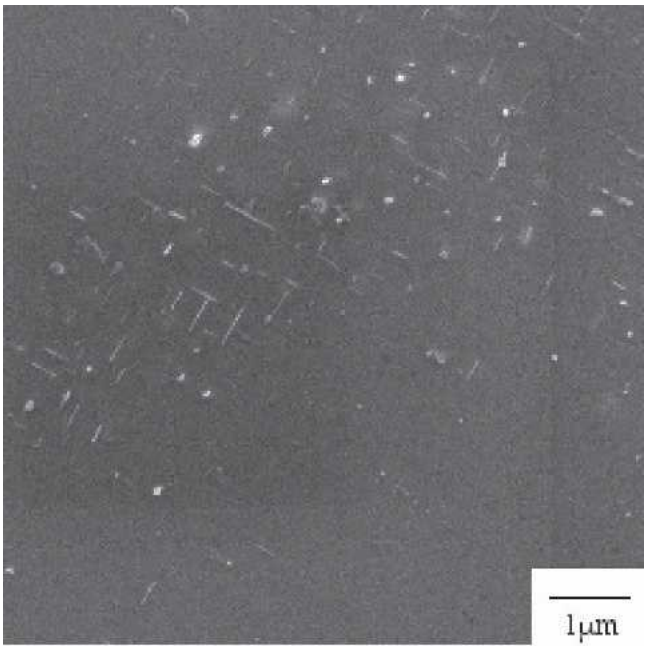

(*b*)

Fig. 3—Micrographs of as-cast Sr-modified D357 alloy showing (*a*) eutectic Si structure and (*b*) Mg_2Si needles in the dendritic region of the Al matrix.

needlelike morphology and is precipitated along favorable crystallographic <100> direction.[12,13] The length of the Mg_2Si particles ranges from 700 to 2000 nm. In addition to needles, few spherical Mg_2Si particles are also observed. The size of Mg_2Si particles is greater in the Sr-modified alloy as compared to the unmodified alloy.

1. *Dissolution of Mg_2Si particles*

The effect of solution heat treatment on dissolution kinetics of Mg_2Si particles using the FB is shown in Figures 4(a) through (c). The number density of Mg_2Si particles in the as-cast and solution-heat-treated condition at 543 °C for 15 and 30 minutes are 0.59, 4.12, and 0.23 μm^2, respectively. The number density increases significantly after 15 minutes of solution heat treatment in the FB as compared to the as-cast condition. The increase in number density of Mg_2Si particles after 15 minutes of solution heat treatment is due to the fragmentation of Mg_2Si needles into small spherical particles. In the as-cast condition, the Mg_2Si particles are mostly needle shaped with lengths ranging from 700 to 2000 nm. In contrast, Mg_2Si particles after 15 minutes of solution heat treatment are mostly spherical in shape with diameters ranging from 20 to 60 nm, and a few needlelike particles whose lengths are about 300 to 500 nm. The formation of spherical particles on solution heat treatment for 15 minutes suggests that Mg_2Si particles undergo fragmentation through neck formation due to curvature effects, as described by Rayleigh's criteria.[14] It should be noted that upon solution heat treatment for 15 minutes, although there is a significant increase in the number density of Mg_2Si particles *vis-à-vis* in the as-cast condition, the volume fraction of Mg_2Si particles does not change significantly. This indicates that the dissolution of Mg_2Si into the Al matrix takes place in two stages: (1) fragmentation of the needles into small spherical particles and (2) dissolution of spherical particles into the Al matrix. After 30 minutes of solution heat treatment, the number density of Mg_2Si is negligibly small and no needle-shaped particles were observed. Similar observations were made in the unmodified D357 alloy. No significant difference is observed in the dissolution kinetics of Mg_2Si particles due to Sr addition in D357 alloy.

2. *Effect on morphology of eutectic Si*

The effect of solution heat treatment on microstructure using the FB *vs* the CF at 543 °C on unmodified D357 is shown in Figures 5(a) through (e). The Si flakes start to fragment to finer Si particles with reduced angularity at the edges within 15 minutes of solution heat treating in the FB (Figure 5(b)); and on further solution heat treating to 120 minutes (Figure 5(c)), the coarsening of eutectic Si takes place through Ostwald ripening. In general, the FB-processed alloy exhibits faster fragmentation and spherodization kinetics as compared to the CF-processed alloy.

The effect of solution treatment on Sr-modified D357 alloy in the FB and the CF at 543 °C is shown in Figures 6(a) through (e). The modification has a strong influence on spherodization and coarsening kinetics of Si particles in the D357 alloy. Figures 6(b) and (c) show optical micrographs of Sr-modified D357 alloy, solution treated using the FB for 15 and 120 minutes, respectively. The eutectic Si is significantly spherodized within 15 minutes of solution heat treatment using the FB. Further solution heat treatment has little effect on the sphericity of Si particles. In contrast, the CF solution-treated alloy exhibits slower fragmentation and spherodizing kinetics. The high spherodizing and coarsening rate of eutectic Si in FB solution-treated alloy is due to the rapid heat transfer rate. The high heating rate experienced by the work piece in the FB enhances fragmentation and spherodization kinetics of the eutectic Si through generation of thermal stresses owing to the thermal mismatch between the eutectic Si and the primary Al. The coefficient of thermal expansion of Si (3.61 μm/m °C) is an order of magnitude

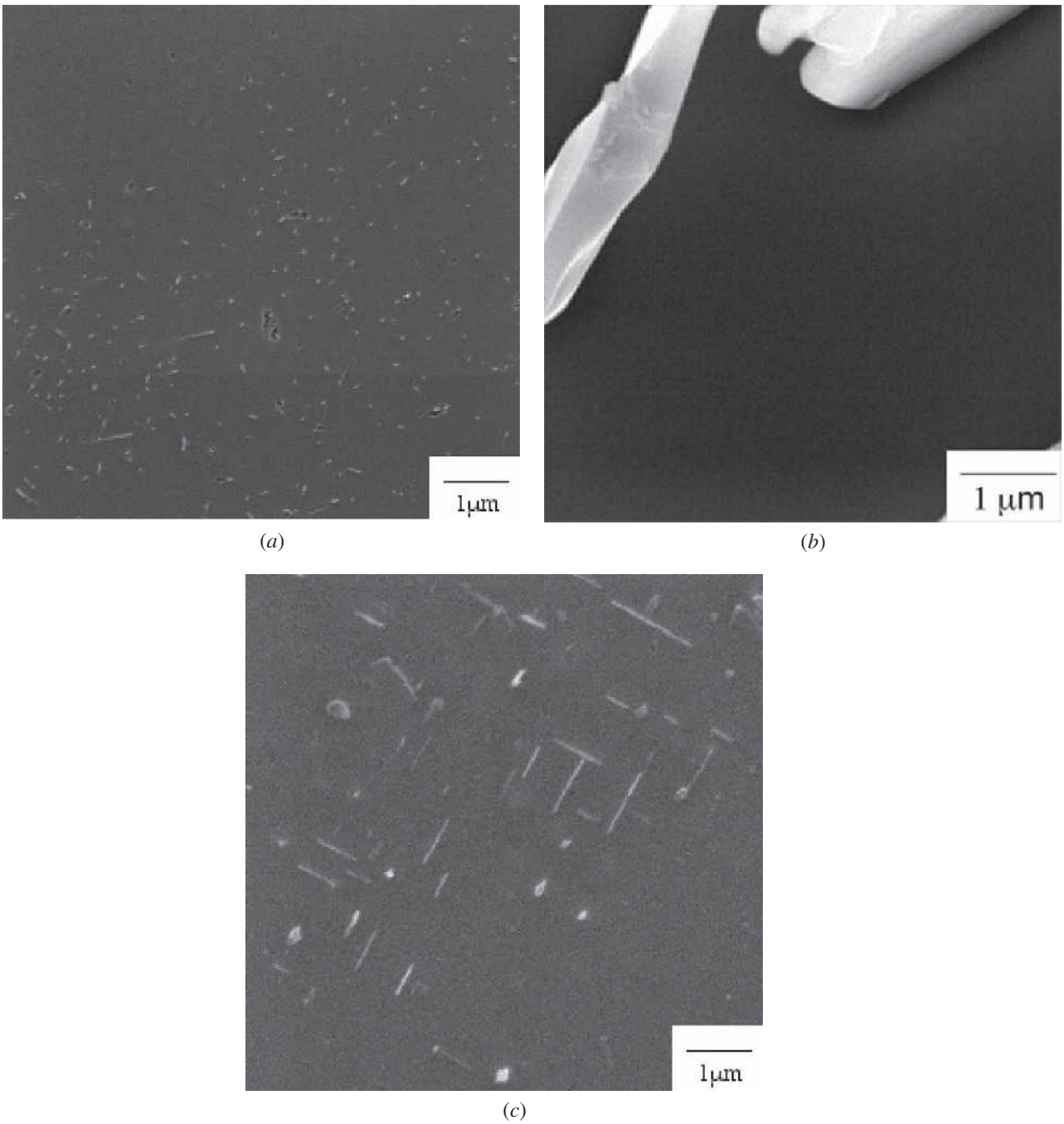

(*a*) (*b*) (*c*)

Fig. 4—Effect of solution heat treatment on dissolution of Mg_2Si particles using the FB at 543 °C for (*a*) 15 min, (*b*) 30 min, and (*c*) as-cast Sr-modified D357 alloy.

lower than that of the primary Al (25.5 μm/m °C) at 250 °C. These thermal stresses induce thermal elastic strains on the eutectic Si and the Al matrix. Accordingly, there can be two possible situations. (1) If the thermal strain exerted on the Si particles exceeds the fracture strain of the Si particles, then fragmentation of Si particles *via* brittle fracture will occur. (2) If the thermal strain is below the fracture strain of the Si particles, then the particles will not fragment, but will enhance the coarsening kinetics through a decrease in elastic and surface energies. The decrease in elastic and surface energies is the driving force for fragmentation and coarsening of the eutectic Si particles.[15,16] Both of these driving forces are dependent on the diffusivity of Si in the Al matrix, which has a higher value, when the phases are in a strained state.

The variation in the eutectic Si particle size as a function of solution heat treatment time for unmodified and modified D357 alloy using both FB and CF is shown in Figures 7(a) and (b), respectively. As expected, the size of eutectic Si increases on solution heat treatment in both unmodified and Sr-modified alloys. In general, the increase in eutectic Si size in the FB-treated alloy is greater than that for the CF-treated

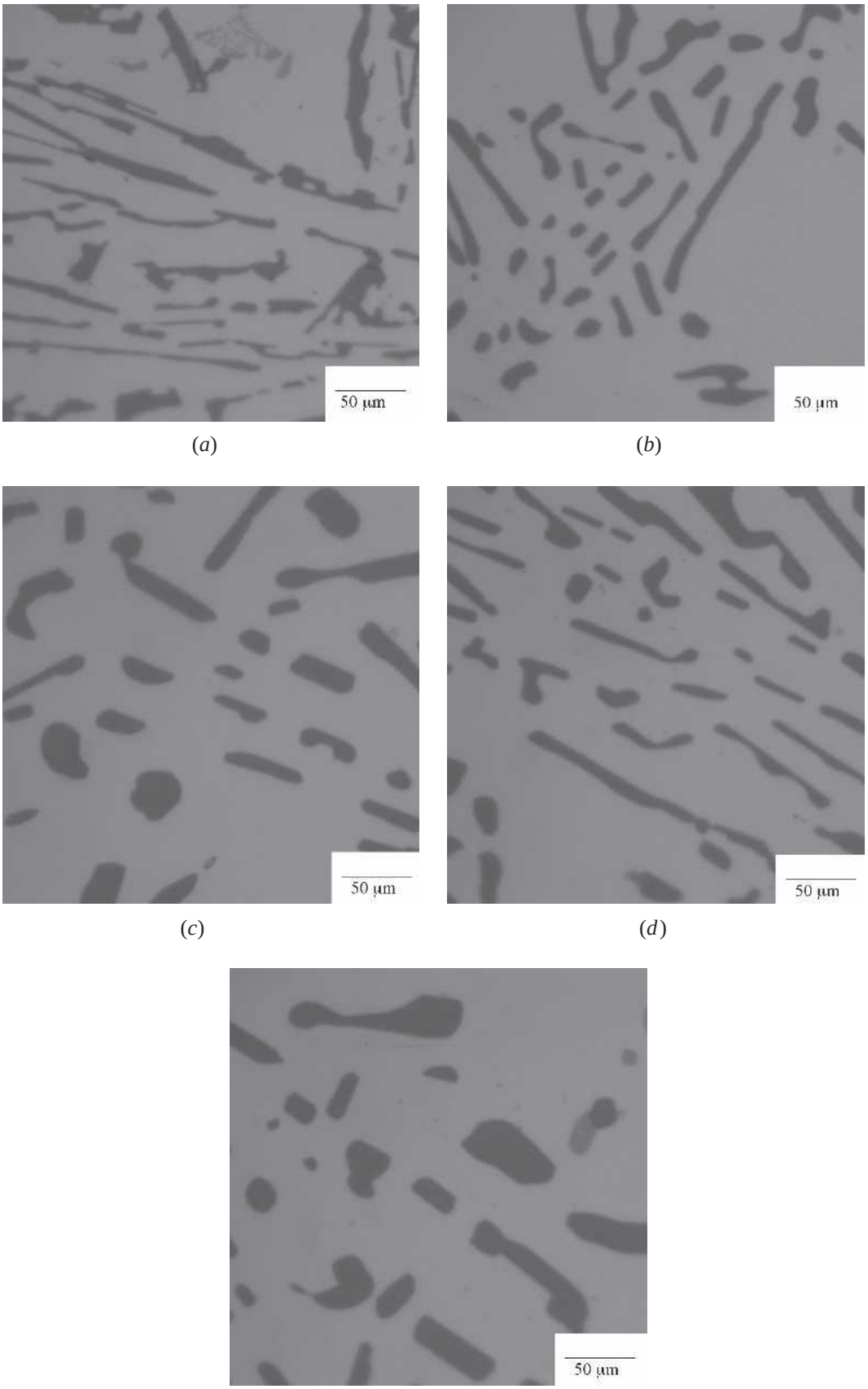

Fig. 5—Optical micrographs of unmodified D357 alloy: (*a*) as cast, (*b*) solution treated at 543 °C for 15 min in FB, (*c*) solution treated at 543 °C for 120 min in FB, (*d*) solution treated at 543 °C for 120 min in CF, and (*e*) solution treated at 543 °C for 540 min in CF.

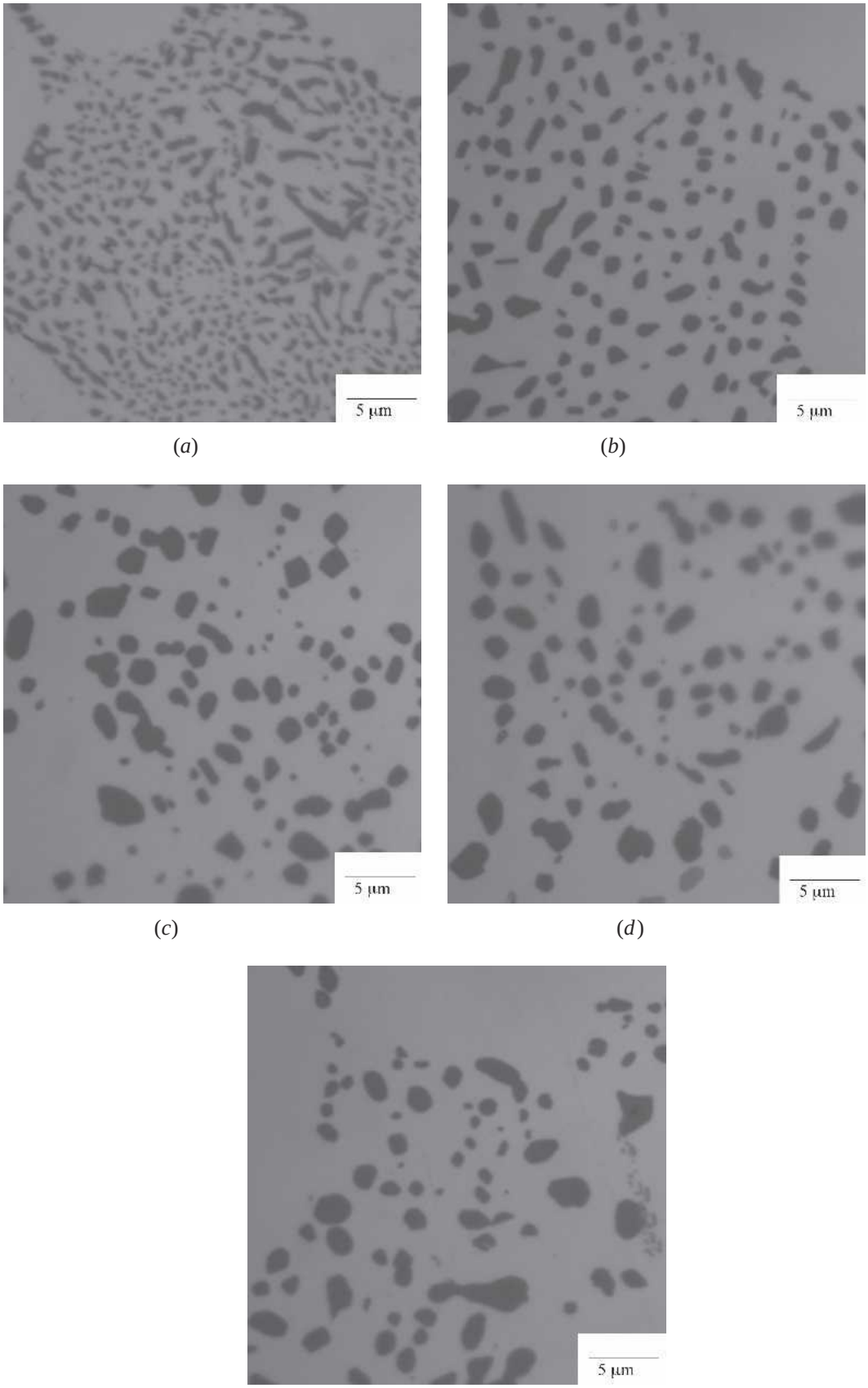

Fig. 6—Optical micrographs of Sr-modified D357 alloy: (*a*) as cast, solution treated at 543 °C for (*b*) 15 min in FB, (*c*) 120 min in FB, (*d*) 120 min in CF, and (*e*) 540 min in CF.

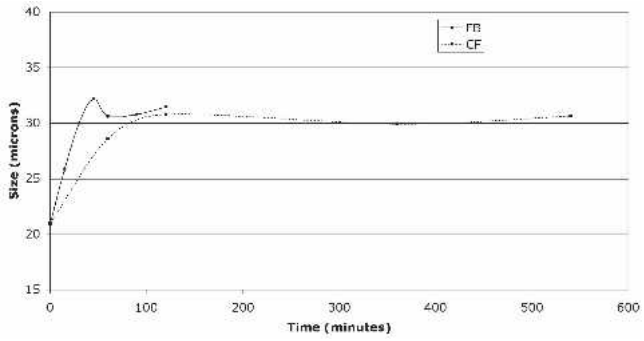

(*a*)

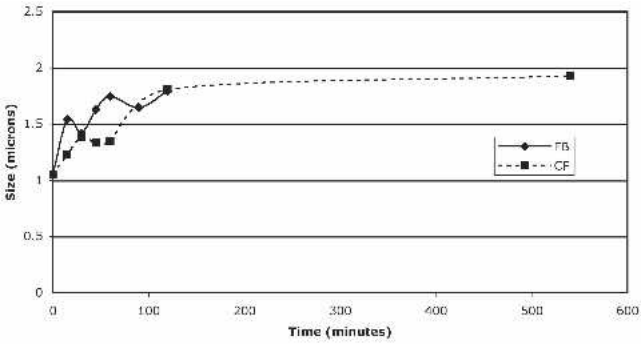

(*b*)

Fig. 7—Change in mean particle size of eutectic Si with solution HT time of (*a*) unmodified D357 alloy and (*b*) Sr-modified D357 alloy.

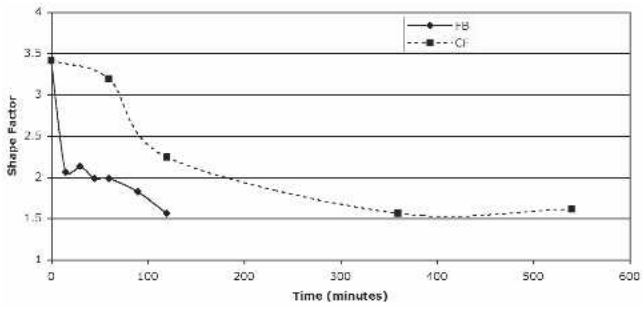

(*a*)

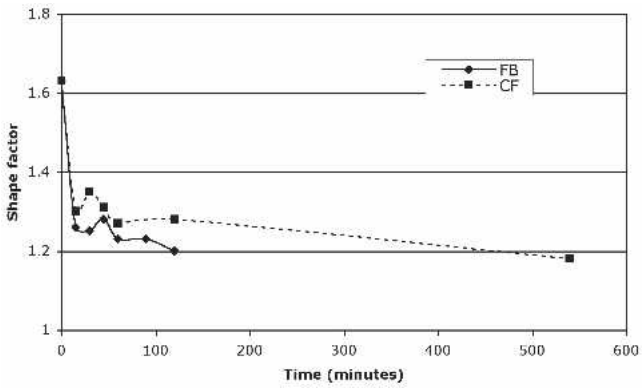

(*b*)

Fig. 8—Change in mean SF of Si particles with solution HT time of (*a*) unmodified D357 alloy and (*b*) Sr-modified D357 alloy.

alloys (both unmodified and modified). In the case of the unmodified alloy, the size increases from 20.96 μm in the as-cast condition to 30.61 μm within 60 minutes when solution heat-treated using the FB. Beyond 60 minutes, no significant change was observed. On the other hand, it took 120 minutes in the CF to attain a size similar to that attained by the FB-treated alloy in 60 minutes. As compared to the unmodified alloy, the Sr-modified alloy showed relatively faster coarsening kinetics. The size of eutectic Si increases from 1.05 μm in the as-cast condition to 1.54 μm when treated for 30 minutes with the FB. Beyond 30 minutes of solution heat treatment in the FB, the change in size of eutectic Si was marginal. The rate of increase in size of eutectic Si is less in CF *vis-à-vis* FB.

The variation in the SF of eutectic Si with solution heat-treatment time using FB and CF for both unmodified and Sr-modified alloys is shown in Figures 8(a) and (b), respectively. As expected, the SF decreases with an increase in solution heat-treatment time. In the case of the unmodified D357 alloy, the SF changes from 3.19 in the as-cast state to 1.98 when solution heat treated for 60 minutes using the FB. Beyond 60 minutes, the decrease in the SF was marginal. As compared to the FB-treated alloy, the CF-treated alloy showed relatively slow spherodizing kinetics. In modified alloy, the SF reduces from 1.63 in the as-cast state to 1.25 and 1.35 after solution heat treatment for 30 minutes using FB and CF, respectively.

In general, spherodization kinetics of eutectic Si in Sr-modified alloy is greater than those in unmodified alloy. Similar observations have been reported elsewhere.[1,17] Both spherodization and coarsening are surface energy driven phenomena; *i.e.*, the system tries to minimize the surface energy through spherodization. It has been reported that morphological changes of eutectic Si take place *via* Si fragmentation due to interfacial instability and their subsequent spherodization and coarsening.[17] It is well known that interfacial stabilities cannot occur readily in platelike (unmodified) eutectic Si particles,[1] and, consequently, the structure is resistant to spherodization. On the contrary, fibrous eutectic Si particles in Sr-modified alloys are susceptible to shape perturbation and consequently particles are easily fragmented.

The standard deviation (SD) in the measured particle size and SF for unmodified and Sr-modified D357 alloys are given in Tables III and IV respectively. It is interesting to note that for Sr-modified alloy, the SD in size increases with increasing solutionizing time of both FB- and CF-treated alloy. This is because coarsening takes place due to Ostwald ripening, where the coarser particle grows at the expense of smaller particles. Consequently, fine particles become smaller and coarse particles grow larger, resulting in greater SD in size. In general, the SD in size of the FB solution heat-treated alloy is greater than the CF-treated alloy. In contrast, the SD in size does not change significantly in the unmodified alloy for both FB- and CF-treated alloy as compared to the as-cast condition. This is due to relatively slow coarsening kinetics of eutectic Si in the unmodified alloy. As expected, the SD in SF decreases with increasing solutionizing times for both FB- and CF-treated alloys (both unmodified and Sr modified). This is because solution heat-treatment results in spherodization of eutectic Si, and with increasing solutionizing times, the sphericity of Si particles increases. In general, the SD in the SF of the FB solutionized alloys (both modified and Sr modified) is smaller than that in the CF-treated alloys.

Table III. SD in the Eutectic Si Particle Size and SF for the Unmodified D357 Alloy

		Solutionizing Time (min)								
Parameter	Processing	0	15	30	45	60	90	120	360	540
SD in size (μm)	FB	3.86	2.47	3.4	4.47	3.5	3.4	4.13	—	—
	CF	3.86	—	—	—	3.96	—	3.65	4.8	4.93
SD in SF	FB	3.21	1.17	1.36	1.25	1.24	0.87	1.07	—	—
	CF	3.21	—	—	—	2.9	—	1.6	0.79	0.95

Table IV. Standard Deviation in the Eutectic Si Particle Size and SF for the Sr D357 Alloy

		Solutionizing Time (min)							
Parameter	Processing	0	15	30	45	60	90	120	540
SD in size (μm)	FB	1.55	1.86	1.94	1.85	1.96	2	2.29	—
	CF	1.55	1.62	1.49	1.73	1.55	—	2	2.09
SD in SF	FB	1.16	0.51	0.52	0.42	0.37	0.38	0.4	—
	CF	1.16	0.66	0.55	0.56	0.37	—	0.37	0.42

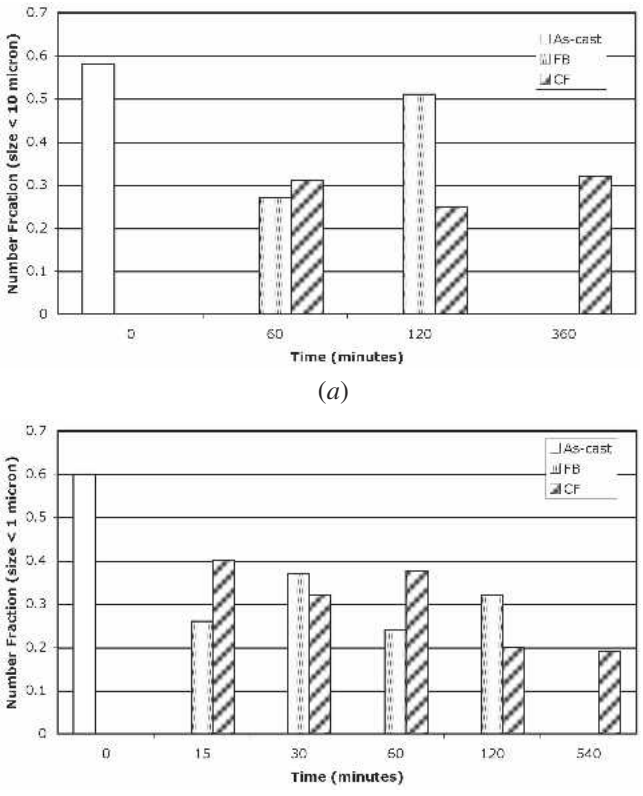

(*a*)

(*b*)

Fig. 9—Variation of number fraction of eutectic Si with solution heat-treatment time at 543 °C in FB and CF of (*a*) unmodified D357 alloy with size less than 10 μm and (*b*) Sr-modified D357 alloy with size less than 1 μm.

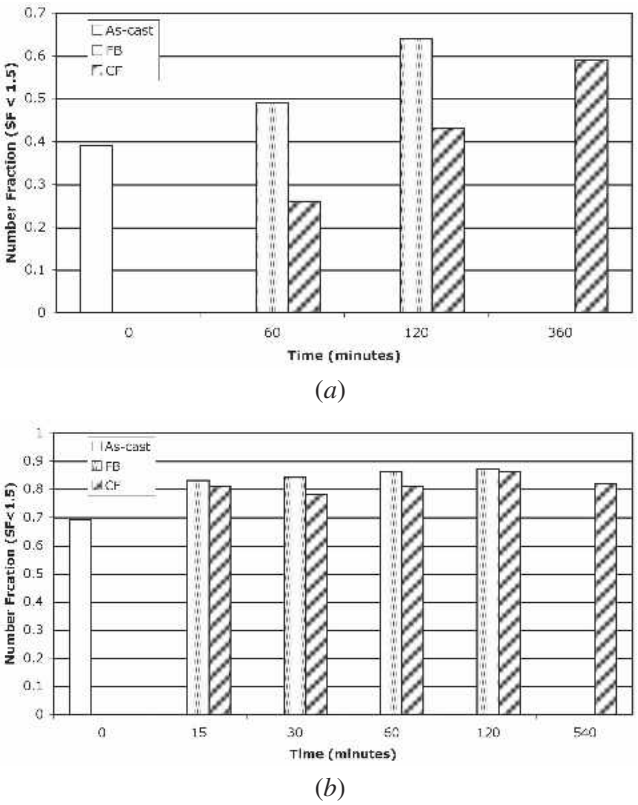

(*a*)

(*b*)

Fig. 10—Variation of number fraction of eutectic Si (SF $<$ 1.5) with solution heat-treatment time at 543 °C in FB and CF for (*a*) unmodified D357 alloy and (*b*) Sr-modified D357 alloy.

The number fractions of eutectic Si particles, with SF less than 1.5 as a function of the solution heat treating time at 543 °C for both unmodified and Sr modified alloys, are shown in Figures 9(a) and (b), respectively. The number fraction of Si particles with SF less than 1.5 increases from 0.34 in the as-cast condition to 0.55 for 15 minutes of solution heat treatment in the FB at 543 °C. Further increases in process time did not lead to any noticeable change in the number fraction of Si particles with SF less than 1.5. Sixty minutes of solution heat treating was required in CF to achieve similar number fractions (0.6 to 0.7) of Si phase with a SF less than 1.5. This reflects that prolonged solution heat treatment has little effect on spherodization kinetics. Moreover, results indicate that the kinetics and effectiveness of fragmentation and spherodization of Si are greater in the FB than with the CF.

The number fractions of eutectic Si with size less than 1 μm (in Sr modified) and less than 10 μm (in unmodified alloy) are shown in Figures 10(a) and (b), respectively. The number fraction of eutectic Si with size less than 1 μm in

Sr-modified alloy decreases with solution heat-treating time. This indicates that the coarsening of eutectic Si takes place *via* Ostwald ripening, where larger particles grow at the expense of smaller particles.

The mechanism of eutectic Si fragmentation and its morphological evolution as a result of heat treatment differs when comparing CF- and FB-processed metal parts. Cylindrical samples of 70-mm length and 38-mm diameter were placed in the FB for 4 minutes and in the CF for 30 minutes; both furnaces were stabilized at 543 °C. The times of 4 and 30 minutes were sufficient for the samples to attain the solution heat-treatment temperature. Figures 11(a) through (d) are SEM micrographs of Sr-modified D357 alloy processed in the FB for 4 minutes. Figures 11(a) through (c) are representative of the fracture of the Si eutectic observed during the FB heat treatment; the effect of rapid heat treatment on eutectic Si located close to the periphery of a dendrite is seen, while Figure 11(d) shows Si particles at the center of the eutectic region. It can be noted that the eutectic Si (Figures 11(a) through (c)) undergoes fragmentation *via* brittle failure (as evidenced by particle cracking) due to the differential thermal stress generated across the Si particle. Thermal stresses are produced due to the rapid heating rate in the FB. In addition, eutectic Si particles (particularly at the center of the eutectic region) undergo rapid fragmentation *via* neck formation (Figure 11(d)) due to curvature effects (Rayleigh's criteria).[5] In contrast, the eutectic Si undergoes fragmentation only *via* neck formation during CF processing (Figure 11(e)). Thus, the fragmentation mechanism of eutectic Si in the FB-processed alloy is of mixed type comprising both brittle fracture and rapid kinetics of neck formation and its propagation, whereas in the CF-processed alloy, it is through relatively slow kinetics of neck formation and their subsequent propagation. The driving forces for Si spherodization during solution heat treatment are as follows: (1) decrease in interfacial energy and (2) decrease in elastic strain energy. The former is due to the surface tension effect and the latter is due to the thermal mismatch between the particle and the matrix. The elastic strain energy is a function of thermal strain, which is greater in the FB-treated alloy owing to its rapid heating. In contrast to this, the slow heating rate in CF gives sufficient time for the atoms to diffuse and thereby reduce thermoelastic strains. The amount of thermal stress generated at the eutectic Si particle/Al interface due to thermal mismatch at solution heat-treatment temperature can be estimated on the basis of the following model.[19]

Assuming a single spherical elastic particle in an elastic matrix, Brooksbank *et al.*[20] have reported that the maximal shear stress, τ_M, that acts in planes oriented at 45 deg with respect to the radial vector of the sphere, is given by

$$\tau_M = \frac{3}{2} \frac{(\alpha_2 - \alpha_1)(T_a - T_f)}{\left[\frac{(1 + \nu_2)}{E_2} + \frac{2(1 - 2\nu_1)}{E_1}\right]} \frac{R^3}{r^3} \qquad [1]$$

where indices 1 and 2 refer to the particle and the matrix, respectively, and

$T_a - T_f$ = temperature difference from stress free state,
α = mean coefficient of thermal expansion over $T_a - T_f$ range,
E = Young's modulus,
ν = Poisson's ratio,
R = radius of particle, and
r = distance from the center of the inclusion.

In the case of the Al-Si system, by taking,[19] $\alpha_1 = 2.6 \times 10^{-6}$, $\alpha_2 = 22.7 \times 10^{-6}$; $E_1 = 165$ GPa, $E_2 = 70$ GPa, $\nu_1 = 0.22$, $\nu_2 = 0.34$, $T_a - T_f = 20$ K, dimensional factor $(R/r) = 1$, Zhou *et al.*[19] showed that the maximal shear stress at the interface that would be induced by a temperature change of 20 °C amounts to 23 MPa. During solution heat treatment, the temperature change ($T_a = 25$ °C, and $T_f = 543$ °C) is 518 °C. Therefore, considering 518 °C as the value of the temperature change ($T_a - T_f$) in Eq. [1], and considering the values for the other parameters as given previously, the calculated value of the maximal shear stress is 596 MPa. This value of the calculated shear stress (596 MPa) is less than the fracture stress of the Si particle, which is generally on the order of 4000 MPa.[21] However, the model is based on the assumption that the Si particle is spherical and the dimensional factor (R/r) is 1. The Si particles are neither spherical nor isolated in castings and have a (R/r) value ranging from 2 to 10. A significant fraction of the Si particles have a ratio or R/r larger than 6. By using Eq. [1], it can be seen that the maximal shear stress will exceed the fracture stress of the Si particle (~4000 MPa) for those that have R/r value larger than 6.7, thus leading to particle fracture. Moreover, the estimation of τ_M under elastic condition is a rough approximation because of the stress relaxation caused by dislocation movements. Local plasticity occurs in the vicinity of the particle/matrix interface, as has been observed in the case of metal matrix composites.[20]

The heating rate plays an important role in the microstructural evolution during solution heat treatment. In CF, owing to the low heating rate (0.6 °C/s), dislocation moves in the Al lattice during the heat-up stage and relaxes thermal stresses on Si particles. In contrast, in the FB due to the high heating rate (5.94 °C/s), there is no opportunity for stress relaxation. Hence, the effect of heating rate on generation of thermal stresses as discussed previously explains the reason for cracking of the Si particles during the heat-up stage (Figure 11(a)) and for the fast coarsening and spherodizing rate of Si particles at the initial stages of solution treatment (less than 60 minutes) in the FB-treated alloys. During prolonged solution heat treatment, the thermal stress (δ_T) in the FB-treated alloys is reduced significantly, and hence, not much difference is observed between the microstructures of the FB- and the CF-treated alloys when solutionized for 2 hours or more.

3. *Effect on Fe-rich intermetallics*

The effect of solution heat treatment at 543 °C in the FB on Fe-rich intermetallics is shown in Figures 12(a) through (c). The EDX analysis revealed that the Fe-rich phase is π phase, though the equilibrium phase diagram predicts the coexistence of both π and β phases for D357 alloy at 543 °C. This is either due to the slow kinetics of transformation or the influence of Be, which stabilizes π phase over β phase. Beryllium has been reported to stabilize the π phase.[18] On solution heat treatment in the FB, the π phase fragments to smaller particles with reduced angularity. The fragmentation takes place *via* neck formation. The complete dissolution of π phase was not observed even during prolonged solution heat treatment for 120 minutes.

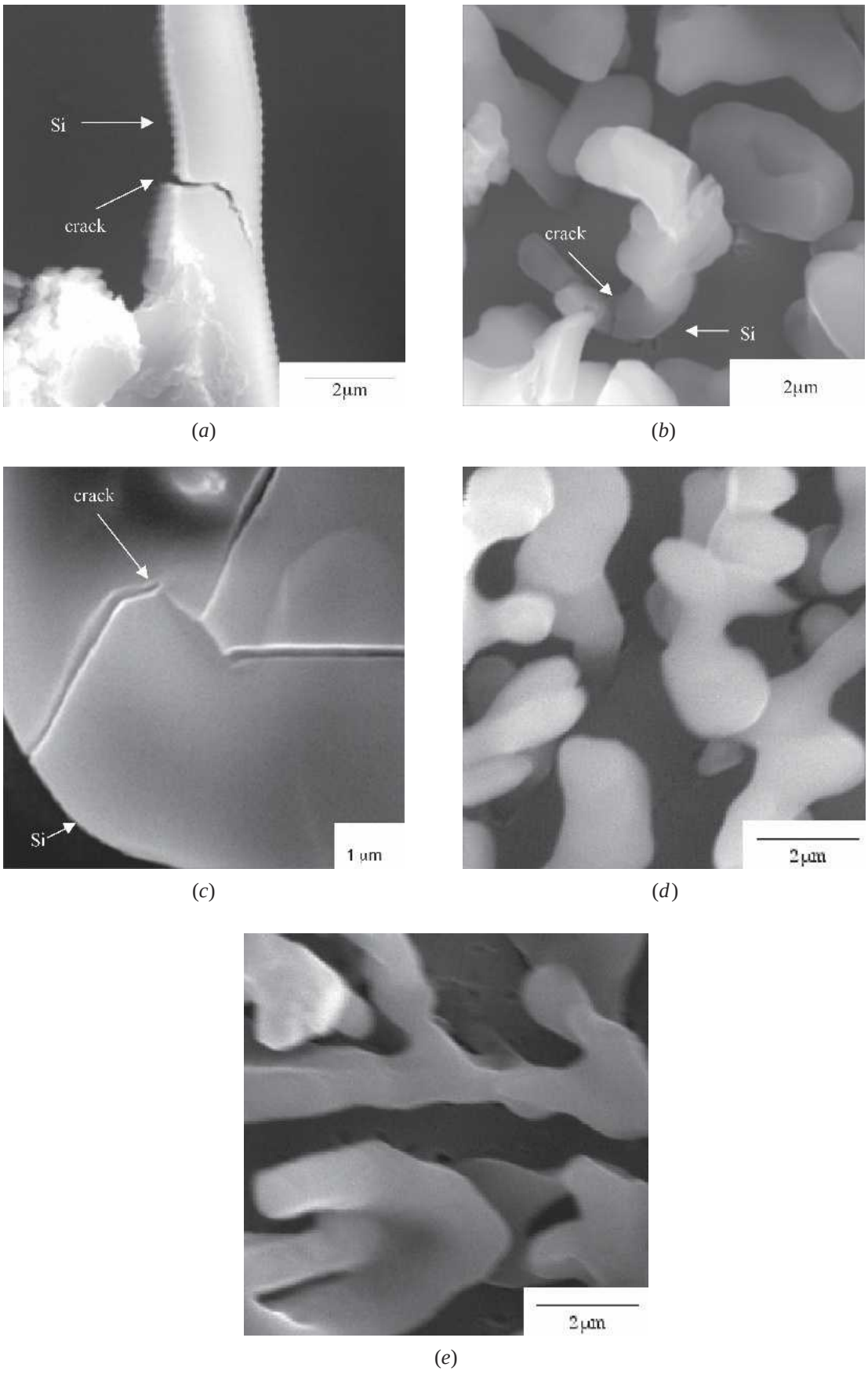

Fig. 11—SEM micrographs of Sr-modified D357 alloy placed in the FB for 4 min (ramp-up time) showing (*a*) through (*c*) fractured Si particles, (*d*) Si particles exhibiting neck formation during FB treatment, and (*e*) Si particles showing negligible change placed in CF furnace for 30 min (ramp-up time).

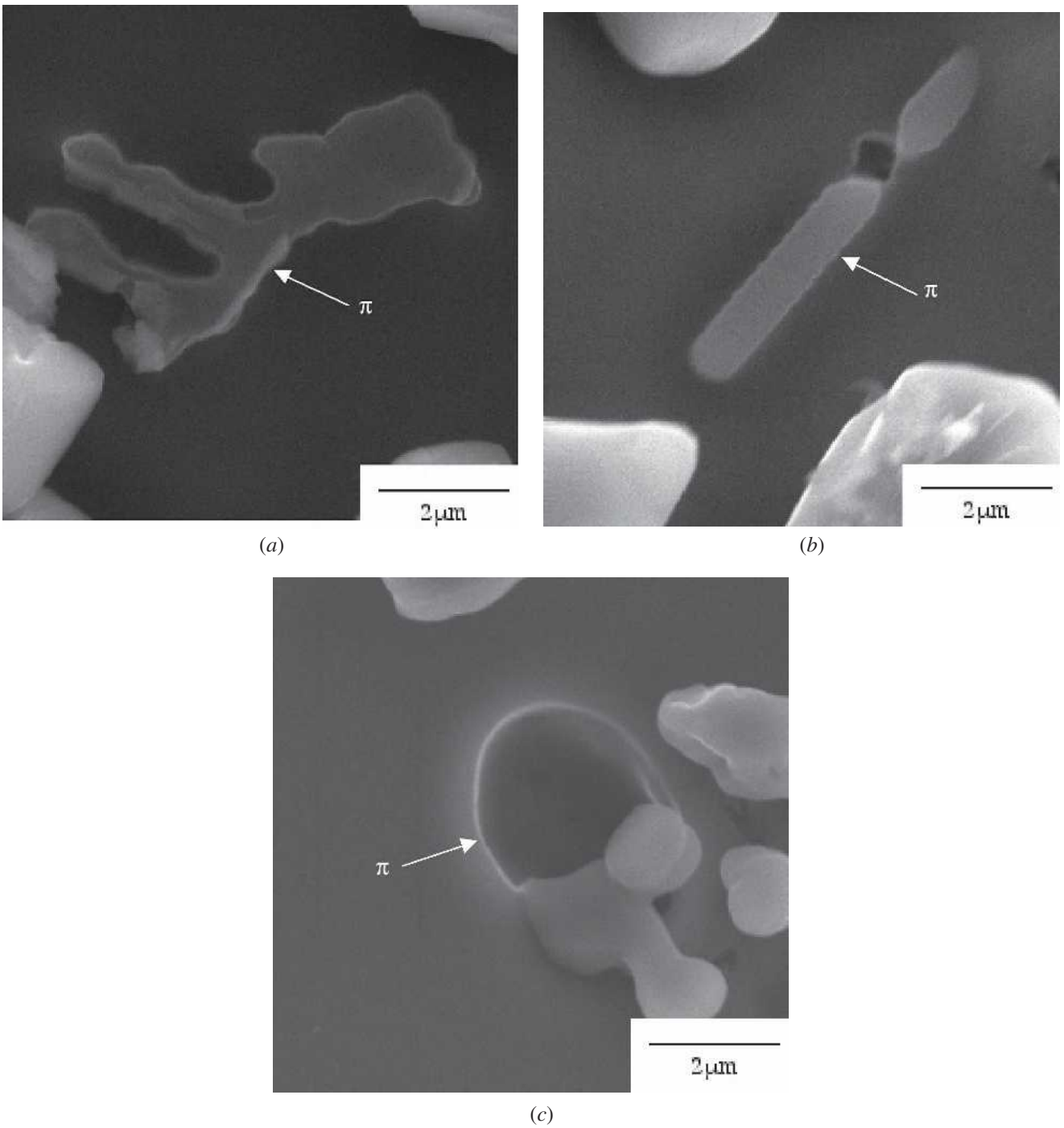

Fig. 12—SEM micrographs showing the effect of solution heat treatment on π phase in Sr-modified D357 alloy: (*a*) as-cast condition, (*b*) solution heated treated at 543 °C for 1 h in FB, and (*c*) for 2 h.

B. *Thermal Analysis*

Thermal analysis was conducted on D357 alloy to understand the role of heating rate on physical/phase transformation(s) during various stages of heat treatment. Figures 13(a) and (b) show thermal analyses of the D357 alloy during solution heat treatment using the FB in a static state (*i.e.*, nonfluidizing state) and the CF, respectively. Note that the thermal profile in the FB was monitored when the bed was in a static condition and hence, the heating rate is relatively low compared to when the bed is in a fluidizing state. It was necessary to carry out the TA in a static FB because data could not be acquired without fluctuations in the fluidized state; no useful TA (first derivative) could be conducted on data mired with fluctuations.

Solution heat treatment in the FB results in an exothermic reaction; the exothermic reaction starts at 98 °C and ends at 112 °C in the FB solution-treated alloys, whereas in the CF solution-treated alloy, the exothermic reaction starts at 253 °C and ends at 320 °C. This indicates that the high heating rate in the FB causes the exothermic reaction

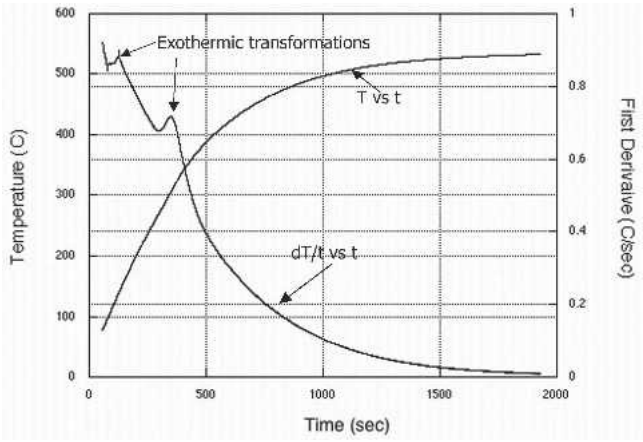

(*a*)

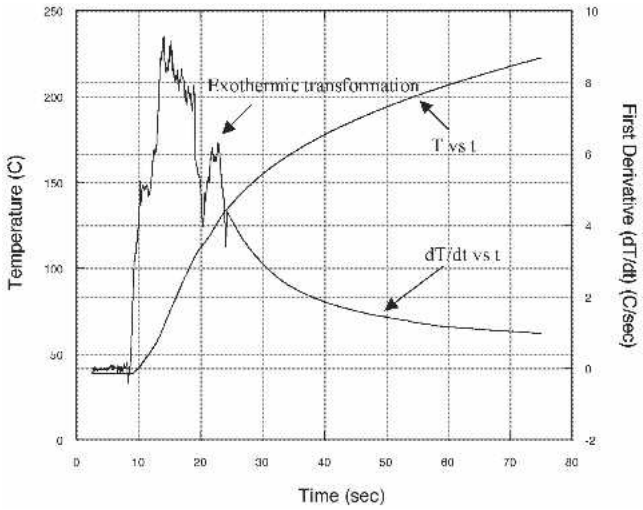

(*b*)

Fig. 13—(*a*) TA of solution heat treatment of D357 alloy in CF. (*b*) TA of solution heat treatment of D357 alloy in FB.

to take place at a much lower temperature than that in CF. In addition, another exothermic reaction takes place during CF solution heat-treated alloy, which starts at 90 °C and ends at about 110 °C, which is likely due to recovery. However, no such transformation was observed in samples processed *via* FB.

The exothermic reaction observed in the temperature range from 90 °C to 110 °C during CF solution heat treatment will lead to the annihilation of point defects resulting in the release of thermal energy; it should be noted that alloys cast under nonequilibrium conditions will contain point defects in the matrix. The second exothermic reaction noted during CF solution heat treatment (in the temperature range of 253 °C to 320 °C) is due to the recrystallization and coarsening of eutectic Al grains. Recrystallization and coarsening are well-known phenomena in wrought Al alloys. The difference in the energy between the strained and unstrained matrices is the driving force for recrystallization and coarsening in mechanically worked wrought alloys. In contrast, cast alloys are not mechanically worked. Therefore, the question here is what is the driving force for the recrystallization in cast alloys? The thermal strain energy generated due to the thermal mismatch between Al and Si is the driving force for recrystallization in cast Al alloys. The coefficient of thermal expansion of Al is an order of magnitude greater than Si.[19] The thermal strain energy generated due to thermal mismatch between Al and Si is calculated using Eq. [1], and the eutectic Al grains are significantly strained during the heat-up stage. In contrast, in wrought alloys, the Al matrix is uniformly strained throughout the matrix due to mechanical working. The differential strain generated by thermal mismatch between Al and Si in the Al matrix of cast alloys is due to the presence of Si particles mostly present in the eutectic region. Therefore, it is reasonable to expect that in the eutectic region (eutectic Al and eutectic Si), the strain will be greater than that in the center of the dendritic region of the primary Al matrix.

The recrystallization of the eutectic grains of the cast Al alloys during solution heat treatment is supported through microstructural observations shown in Figures 14(a) and (b) for Sr-modified D357 alloy solutionized for 60 minutes. The micrographs show coarsened eutectic Al grains formed after recrystallization, which is evidence for the observed exothermic peak during TA in the FB and CF (high-temperature peak). Therefore, there is a fundamental difference in the concept of recrystallization between wrought and cast Al alloys. In cast Al alloys, eutectic grains are more prone to recrystallize, whereas in wrought alloys, the entire Al matrix is recrystallized. In other words, in the case of cast Al alloys, recrystallization is a localized phenomenon limited to the eutectic region, whereas in wrought alloys, it occurs throughout the matrix. The TA of the FB solution heat-treated sample shows that the exothermic transformation as a result of recrystallization takes place at lower temperatures *vis-à-vis* CF-treated samples due to the high heating rate in FB, which generates large thermal stresses. It has been reported that thermal stress is directly proportional to the heating rate.[11] Thermal stress is the driving force for the recrystallization of the eutectic grains; consequently, the transformation temperature is lower when there is a large driving force, *i.e.*, when thermal stresses are large.

C. *Mechanical Properties*

Figures 15(a) through (c) show the variation in ultimate tensile strength (UTS), yield strength (YS), and elongation of unmodified D357 alloy solution treated in the FB and the CF for various intervals. As expected, UTS, YS, and elongation increase with increasing solutionizing times. The superiority of the FB processing (solution heat treating) over the CF with regard to reducing solution heat-treating time is clearly seen. In the case of unmodified alloy, it takes about 15 minutes in the FB to get a reasonably high UTS (275 + MPa) value, whereas using the CF, it takes about 180 minutes to attain the same level of strength. For the unmodified D357 alloy, reasonably good ductility (7 + pct elongation) is achieved only after 60 minutes of solution heat treating in the FB, whereas in the CF, it takes about 3 hours.

Figures 16(a) through (c) show the UTS, YS, and elongation of Sr-modified D357 alloy solution treated in FB and CF. As expected, solution heat treatment leads to significant gain in UTS, YS, and elongation of the alloy. Reasonably good UTS (275 + MPa) and ductility (~12 pct elongation) is achieved within 30 minutes of solution heat treating in the FB. The increase in the UTS and the YS of solutionized alloys is

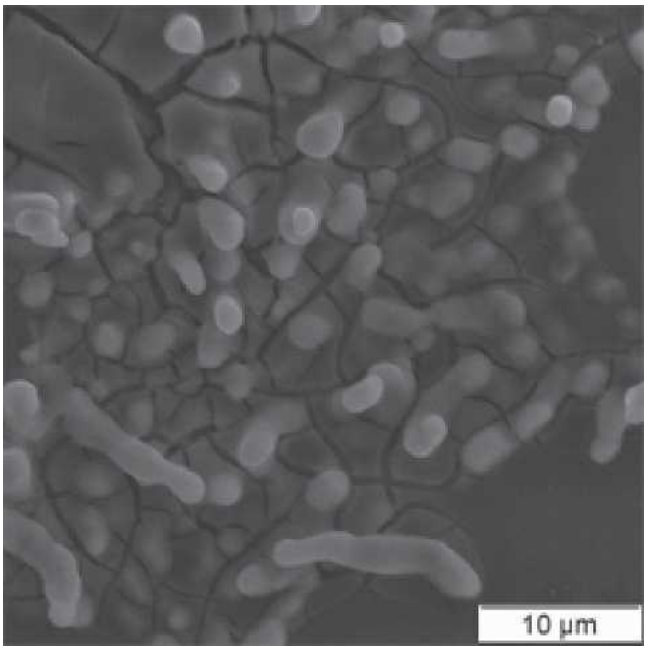

(*a*)

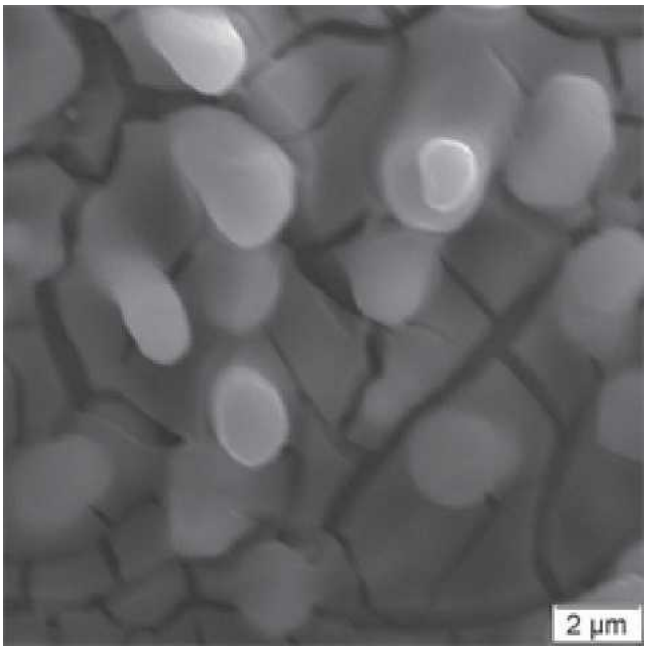

(*b*)

Fig. 14—Deep-etched micrographs of Sr-modified D357 alloy solutionized at 543 °C for 1 h using FB showing recrystallized and coarsened eutectic Al grains at (*a*) 1900 times and (*b*) 5000 times.

due to solid solution strengthening, and the increase in elongation is due to the spherodization of eutectic Si particles. Further, it is clear that Sr modification leads to faster solution heat treating (due to rapid spherodization) through FB *vis-à-vis* CF. Based on the preceding results, the optimum solution heat-treating time using the FB for the Sr-modified alloy is 30 minutes, and that for the unmodified alloy is 60 minutes. In the unmodified D357 alloy, for the 60-minute solution heat-treatment time, an elongation of about 7 pct and a UTS greater than 290 MPa are attained, while for the Sr-modified alloy,

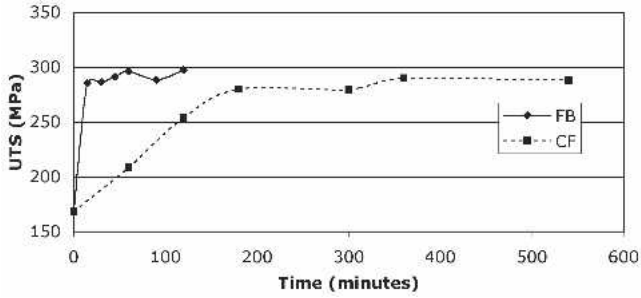

(*a*)

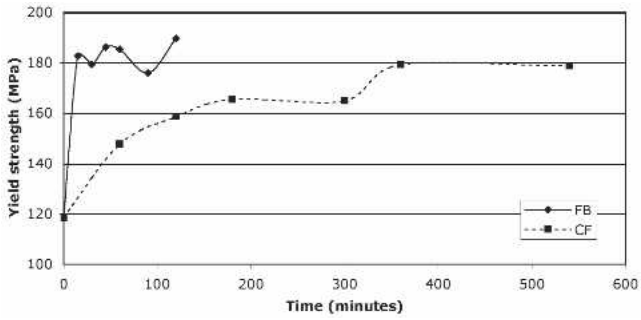

(*b*)

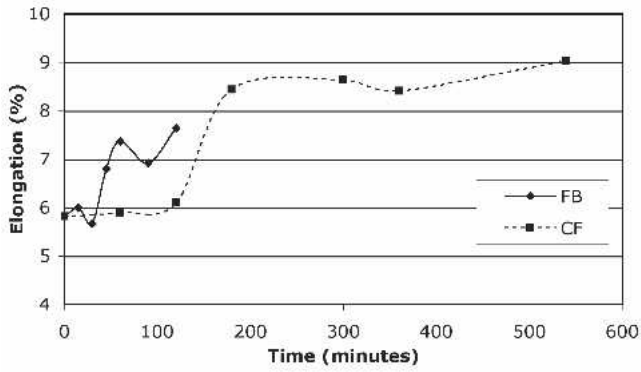

(*c*)

Fig. 15—Effects of solution heat treatment (T4 condition) for unmodified D357 alloy on (*a*) UTS, (*b*) yield strength; and (*c*) elongation.

for the 30-minute solution heat-treatment time, an elongation of 12 pct and UTS greater than 290 MPa are attained.

IV. CONCLUSIONS

1. The heating rate in the FB is greater than in the CF.
2. The high heating rate in the FB results in greater spherodization kinetics of eutectic Si during solution heat treatment than that in the CF.
3. The mechanism of Si fragmentation is through brittle fracture due to thermal mismatch between Al and Si and rapid neck formation in the FB heat-treated castings. In contrast to this, the mechanism of Si fragmentation in alloy solution heat treated using a CF is through relatively slow neck formation and its propagation.
4. Optimum solution heat-treatment times using the FB for unmodified and Sr-modified alloy are 60 minutes and 30 minutes, respectively.

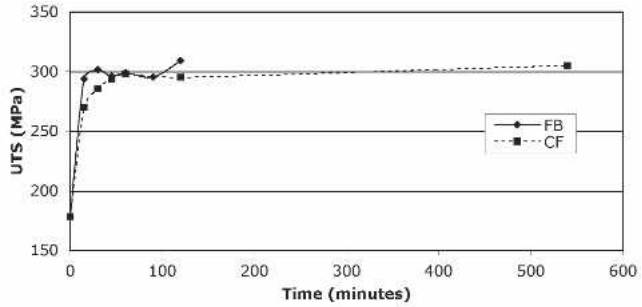

(*a*)

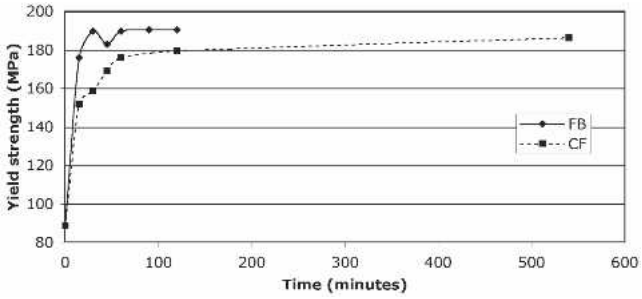

(*b*)

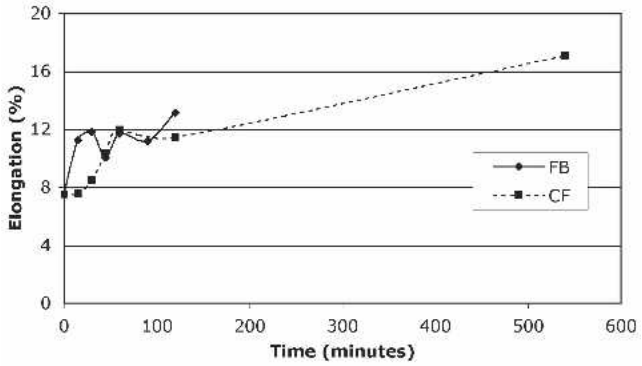

(*c*)

Fig. 16—Effects of solution heat treatment (T4 condition) for Sr-modified D357 alloy on (*a*) UTS, (*b*) yield strength, and (*c*) elongation.

ACKNOWLEDGMENTS

The authors are thankful to Hitchcock Industries (MN) for supplying the alloys for this study. The authors thank the corporate members of the Advanced Casting Research Center of the Metal Processing Institute for their support of this work.

REFERENCES

1. D. Apelian, S. Shivkumar, and G. Sigworth: *AFS Trans*., 1989, vol. 89–138, p. 727.
2. L. Pedersen and L. Arnberg: *Metall. Mater. Trans. A*, 2001, vol. 32A, p. 525.
3. P.N. Crepeau: *AFS Trans*., 1995, vol. 103, p. 361.
4. M. Murayama and K. Hono: *Acta Mater*., 1999, vol. 47 (5), p. 1537.
5. S. Shivkumar, S. Ricci, B. Steenhoff, D. Apelian, and G. Sigworth: *AFS Trans*., 1989, vols. 89–138, p. 791.
6. M.H. Mulazimoglu, A. Zaluska, F. Paray, and J.E. Gruzleski: *Metall. Mater. Tran. A*, 1997, vol. 28A, p. 1289.
7. C.H. Bergman and S.I. Krause: U.S. Patent No. 6,042,369, Mar. 28, 2000.
8. T.O. Mbuya, B.O. Odera, and S.P. Nganga: *Int. J. Cast Met. Res*., 2003, vol. 16 (5), p. 451.
9. D.G. McCartney: *Int. Mater. Rev*., 1989, vol. 34, p. 247.
10. S. Chaudhury, S. Shankar, D. Apelian, and J. Van Wert: *Proc. AFS Aluminum Structural Casting Conf*., Orlando, FL, AFS, Nov. 2–4, 2003.
11. S.K. Chaudhury, L. Wang, and D. Apelian: *AFS Trans*., 2004, vol. 112, pp. 04-055.
12. J.Y. Yao, D.A. Graham, B. Rinderer, and M.J. Couper: *Micron*, 2001, vol. 32, p. 865.
13. J.A. Sigmund: *Metall. Mater. Trans A*, 1995, vol. 26A, p. 1931.
14. E. Ogris, A. Wahlen, H. Luchinger, and P.J. Uggowitzer: *J. Met*., 2002, vol. 2, p. 263.
15. K. Thornton, N. Akaiwa, and P.W. Voorhees: *Acta Mater*., 2004, vol. 52 (5), p. 1353.
16. K. Thornton, N. Akaiwa, and P.W. Voorhees: *Acta Mater*., 2004, vol. 52 (5), p. 1365.
17. P.Y. Zhu, Q.Y. Liu, and T.X. Hou: *AFS Trans*., 1985, vol. 93, p. 609.
18. F.H. Samuel, A.M. Samuel, H.W. Doty, and S. Valtierra: *Metall. Mater. Trans. A*, 2003, vol. 34A, p. 115.
19. X. Zhou, R. Fougeres, A. Vincent, and J. Phys: *III France*, 1992, vol. 2, p. 2185.
20. D. Brooksbank and K.W. Andrews: *J. Iron Steel Inst*., 1972, vol. 210, p. 246.
21. S.M. Spearing: *Acta Mater*., 2000, vol. 48, p. 179.
22. L. Snugovsky, J.F. Major, D.D. Perovic, and J.W. Rutter: *Mater. Sci. Technol*., 2000, vol. 16, p. 125.